ACS Sustainable Chemistry & Engineering

Research Article

pubs.acs.org/journal/ascecg

Fabrication and Properties of Microencapsulated Paraffin@SiO_2 Phase Change Composite for Thermal Energy Storage

Benxia Li,* Tongxuan Liu, Luyang Hu, Yanfen Wang, and Lina Gao

School of Materials Science and Engineering, Anhui University of Science and Technology, Huainan, Anhui 232001, China

ABSTRACT: In this work, a novel microencapsulated phase change composite of paraffin@SiO_2 was prepared by in situ emulsion interfacial hydrolysis and polycondensation of tetraethyl orthosilicate (TEOS). The as-prepared paraffin@SiO_2 composite was determined by Fourier transformation infrared spectroscope (FT-IR), X-ray diffractometer (XRD), scanning electronic microscope (SEM), and transmission electron microscopy (TEM), respectively. The results showed that the paraffin@SiO_2 composite is composed of quasi-spherical particles with diameters of 200−500 nm. The paraffin is encapsulated in a SiO_2 shell, and there is no chemical reaction between them. The DSC results indicate that the melting temperature and latent heat of the composite are 56.5 °C and 45.5 J/g, respectively. The encapsulation ratio of paraffin was calculated to be 31.7% from the results of the DSC measurements, slightly lower than the loading content (32.5%) of paraffin in the microencapsulated composite from the TGA measurements. The as-prepared paraffin@SiO_2 composite could maintain its phase transition perfectly after 30 melting−freezing cycles, and no leakage of paraffin was observed at 70 °C for 20 min. Moreover, the high heat storage capability and good thermal stability of the composite enable it to be a potential material to store thermal energy in practical applications.

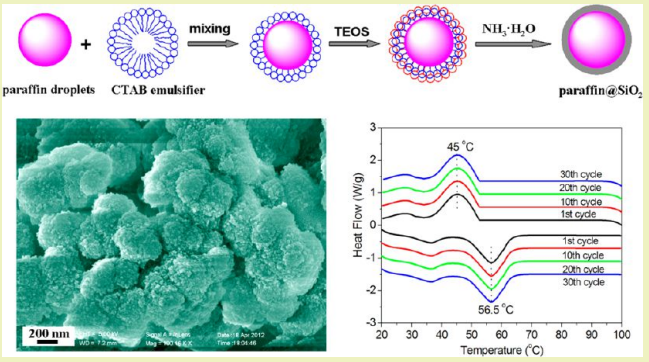

KEYWORDS: *Chemical synthesis, Composite, Microencapsulation, Phase change material, Thermal energy storage*

INTRODUCTION

Because of the shortage in conventional fossil energy and the demand for functional materials in thermal energy management, it is increasingly prevailing to use phase change materials (PCMs) for storing thermal energy and adjusting temperature by storing and releasing large amounts of latent heat during the phase change process.[1−3] PCMs are recognized as the ideal thermal energy management materials with the advantages of high density of latent heat and constant temperature during heat storage/release,[4,5] and they are expected to show broad prospects in the use of solar energy utilization,[6] temperature-regulating greenhouses,[7] homothermal textiles,[8] heat management of electronics,[9] etc. Some organic PCMs, like paraffin and fatty acids,[10−13] have been recommended as favorable PCMs having desirable properties such as high latent heat, congruently melting/freezing, little supercooling, low vapor pressure, nontoxicity, and easy availability. However, the direct utilization of these organic PCMs for heat storage is subject to some restrictions because of their low thermal conductivity and the need of special sealed packages to prevent their leakage during the solid−liquid phase transitions.

In recent years, microencapsulation technology has been developed and thereupon shows a great potential for resolving the problems existing in the utilization of organic solid−liquid PCMs.[14−17] Microcapsules are tiny containers that encapsulate the PCMs as core in a hard shell. Therefore, the microencapsulated PCMs are endowed with many fascinating virtues like having large heat transfer area, preventing the PCMs from reacting with the outside environment and controlling the volume change of the PCMs during phase transitions.[18] As a result, various physical and chemical methods have been developed for preparing the microencapsulated PCMs, such as spray drying,[19] interfacial polymerization,[20] and in situ polymerization.[21] Whereas, most of the reported microencapsulated PCMs use organic polymers as the shell materials which usually release poisonous formaldehyde in the application, causing environmental and health problems.[22,23] Besides, the microencapsulated PCMs containing organic PCMs (paraffin, fatty acids/esters, etc.) and organic polymer shell materials are easily flammable, and their application is therefore severely limited. Therefore, organic−inorganic microencapsulated phase change composites are attracting substantial attention, which has the potential of taking full advantages of organic and inorganic components.

Microencapsulating organic PCMs into inorganic shells has been achieved so far by several different methods including the sol−gel method through an oil-in-water (O/W) emulsion route,[15,24] spray drying technique,[25] and in situ interfacial polycondensation.[16] Especially, the in situ interfacial polycondensation of tetraethyl orthosilicate (TEOS) in O/W

Received: August 20, 2012
Revised: December 13, 2012
Published: January 17, 2013

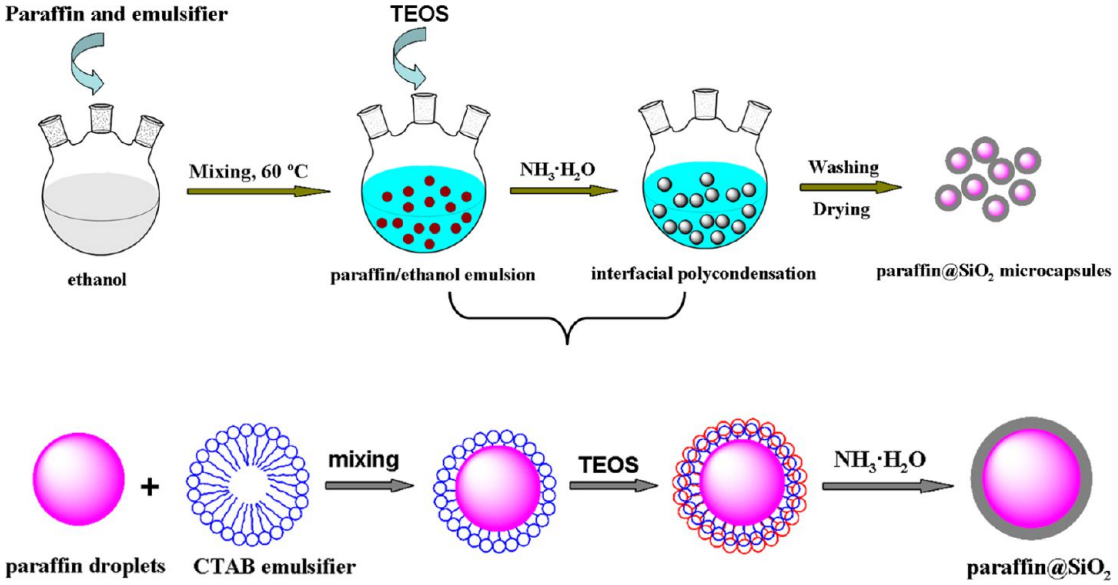

Figure 1. Schematic diagram for the formation of the microencapsulated paraffin@SiO_2 composite via in situ emulsion interfacial hydrolysis and polycondensation.

emulsion for fabrication of organic@SiO_2 microencapsulated PCMs is more attractive because of its easily controllable condition and relatively cheap equipments, and it represents an environmentally kind and user-friendly approach. Herein, a novel microencapsulated PCM with paraffin as core and SiO_2 as shell was prepared by in situ emulsion interfacial hydrolysis and polycondensation of TEOS. The as-prepared composite has an advisable microencapsulated capacity of paraffin, high thermal storage capability, and good thermal stability, indicating that the composite can be used as a potential material to store thermal energy in practical application.

EXPERIMENTAL SECTION

In a typical procedure to prepare the microencapsulated paraffin@SiO_2 composite, paraffin (2 g), cetyltrimethylammonium bromide (CTAB, 1.5 g) and n-amyl alcohol (10 mL) were mixed in absolute alcohol (100 mL) by ultrasonic dispersion in a three-necked flask (250 mL), followed with stirring for 60 min at 60 °C. Then, 10 mL of TEOS was added into the flask dropwise. After stirring the mixture for 30 min at 60 °C, precipitation was initiated by dripping 2 mL of aqueous ammonia (25 wt %). The mixture was then stirred at 60 °C for 2 h. The resultant paraffin@SiO_2 product was washed several times and collected by vacuum filtration to remove the residual reagents and finally dried at 50 °C for 12h. The experiment yield of the resultant paraffin@SiO_2 composite was calculated as 55%.

The X-ray diffraction (XRD) patterns of the samples were carried out on X-ray diffractometer (Shimadzu XRD-6000, Cu Kα radiation), and the FT-IR spectra were recorded on a Nicolet380 from 400 to 4000 cm^{-1} using KBr pellets that were prepared by pressing pellets containing 100 mg KBr and 1 mg of sample. The morphology and microstructure of the microencapsulated paraffin@SiO_2 composite were observed on a field emission scanning electron microscopy (FESEM, JEOL JSM-6700F, Japan) and transmission electron microscopy (TEM, H-7650). Thermal gravimetric analyses (TGA) of the samples using about 5 mg for every sample were carried out on a Shimadzu TA-50 thermal analyzer at a heating rate of 10 °C/min from room temperature to 600 °C in air. The phase change temperature and latent heat of the products were measured using a differential scanning calorimeter (NETZSCH DSC 200 F3). For DSC measurements, about 5.5 mg for every sample was sealed in an aluminum pan for characterization at a heating rate of 5 °C/min under a constant stream of argon at flow rate of 20 mL/min.

The test of thermal storage/release performance was conducted using the constant temperature water bath method.[26,27] The sample was sealed in a homemade aluminum test tube, and a thermocouple was placed in the center of the test tube. The test tube was put into a water bath at a constant temperature of 80 °C, where heat storage was carried out. After the temperatures of the samples achieved 80 °C, the samples were immediately cooled at room temperature, where the samples performed the heat release process. The temperature variations of the samples during these periods were recorded automatically by a data logger with a temperature measuring accuracy of ±1 °C at time intervals of 1 min.

RESULTS AND DISCUSSION

In the present case, the microencapsulated paraffin@SiO_2 composite was fabricated by an in situ emulsion interfacial hydrolysis and polycondensation process of TEOS, and the formation process is shown in the schematic diagram (Figure 1).[28] Paraffin is not soluble in alcohol. When paraffin was dispersed in the ethanol solution containing CTAB as surfactant and n-amyl alcohol as a cosurfactant, a stable paraffin/ethanol emulsion was formed in the reaction mixture, in which the hydrophobic segments of the emulsifiers are oriented into the oil droplets of paraffin, and meanwhile, the hydrophilic segments of them are associated with the ethanol molecules away from the oil phase. As a result, an emulsifier layer is formed to cover the surface of the oil droplets of paraffin. When TEOS was added into the emulsion system, it was captured by the emulsifier layer due to its amphiphilic property, meaning that most of TEOS exists around the oil droplets of paraffin. When the aqueous ammonia was dripped into the emulsion containing paraffin micelles and TEOS, SiO_2 formed via the ammonia-catalyzed hydrolysis and polycondensation of TEOS as eqs 1 and 2 and were synchronously attracted onto the surface of the micelles through an electrostatic interaction between the SiO_2 and CTA^+ chains. As a result, the SiO_2 shell was successfully fabricated onto the surface of the paraffin droplets though such an interfacial hydrolysis and polycondensation process.

dx.doi.org/10.1021/sc300082m | ACS Sustainable Chem. Eng. 2013, 1, 374−380

$$\text{Hydrolysis: } Si(OC_2H_5)_4 + 4H_2O \rightarrow Si(OH)_4 + 4C_2H_5OH \quad (1)$$

$$\text{Polycondensation: } Si(OH)_4 + Si(OH)_4 \xrightarrow{NH_3\cdot H_2O, C_2H_5OH} 2SiO_2 + 4H_2O \quad (2)$$

Chemical compositions of the samples were characterized by FT-IR spectroscopy (Figure 2) and XRD patterns (Figure 3).

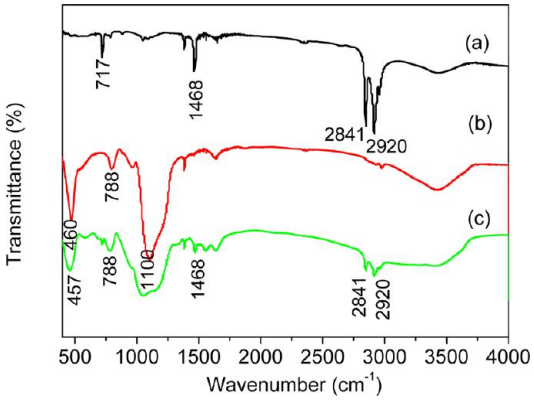

Figure 2. FT-IR spectra of (a) paraffin, (b) SiO_2, and (c) microencapsulated paraffin@SiO_2 composite.

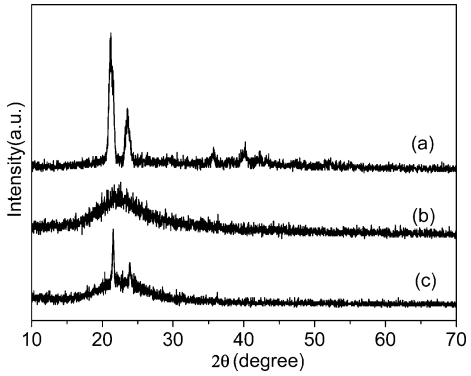

Figure 3. XRD patterns of (a) paraffin, (b) SiO_2, and (c) microencapsulated paraffin@SiO_2 composite.

The FT-IR spectra of paraffin, SiO_2, and the microencapsulated paraffin@SiO_2 composite are shown in Figure 2. In the spectrum of paraffin (Figure 2a), the peaks at 2920 and 2841 cm^{-1} correspond to the stretching vibration of C−H, the peaks at around 1468 cm^{-1} belong to the deformation vibration of $-CH_2$ and $-CH_3$, and the peak at 717 cm^{-1} is due to the in-plane rocking vibration of $-CH_2$. In the spectrum of SiO_2 (Figure 2b), the peaks at 1100, 788, and 465 cm^{-1} are ascribed to the bending vibration of Si−O−Si. The absorption band at 3200−3600 cm^{-1} and around 1630 cm^{-1} represent, respectively, the stretching vibration and bending vibration of functional group of −OH of H_2O adsorbed into the pores of SiO_2.[29] In the spectrum of paraffin@SiO_2 composite (Figure 2c), the peaks assigned to SiO_2 at 1100, 788, and 457 cm^{-1}, and the peaks assigned to paraffin at 2920, 2841, 1468, and 717 cm^{-1} still existed, and no significant new peak is observed, which indicates that the paraffin@SiO_2 composite is just a physical interaction between paraffin and SiO_2. Figure 3 shows the XRD patterns of paraffin, SiO_2, and the paraffin@SiO_2 composite. In Figure 3a, two sharp diffraction peaks at 2θ = 21.17° and 2θ = 23.53° are attributed to the diffractions of (110) and (200) crystal planes of paraffin, respectively (JCPDS No. 40-1995). In Figure 3b, only a broad band at 2θ = 17° ∼ 25° appears in the XRD pattern of pure SiO_2, indicating the SiO_2 sample is amorphous. The XRD pattern of the paraffin@SiO_2 composite (Figure 3c) contains the peaks of paraffin and the broad band of amorphous SiO_2, whereas the peak intensities are relatively lower in comparison with those of pure paraffin and SiO_2. The results suggest that the composite is just the physical combination of paraffin with SiO_2, and no new substance has been produced.

The morphology and microstructure of the microencapsulated paraffin@SiO_2 composite were observed by the SEM and TEM images as shown in Figure 4. A SEM image in Figure 4a shows that the microencapsulated paraffin@SiO_2 composite is composed of quasi-spherical particles with diameters of 200−500 nm, but these particles present some conglutination with each other. The magnified SEM image in Figure 4b reveals that these quasi-spherical paraffin@SiO_2 composite particles have very coarse surfaces, which may be because the rapid diffusion of the $NH_3\cdot H_2O$ molecules accelerated the hydrolysis and polycondensation of TEOS toward the surface of the paraffin droplets, and the SiO_2 colloidal particles cannot form a smooth and compact shell on the paraffin core.[28] The results from TEM images (Figure 4c,d) are consistent with those observed from SEM images and further indicate that the paraffin@SiO_2 composite is composed of paraffin core with diameters in 100−200 nm and SiO_2 shell with uneven thickness. On the basis of all of the above FT-IR spectra, XRD patterns, and SEM−TEM observations, it can be seen that the microencapsulated paraffin@SiO_2 shape-stabilized composite has been obtained by the present method. Although the well-defined spherical morphology was obtained in the previous report,[16] the thermal storage capabilities of the microencapsulated composites drastically decreased because the chemical interaction between organic PCM and the inorganic shells changes the properties of the organic PCM. Whereas, the present paraffin@SiO_2 composite exhibits a higher thermal storage capability (discussed next) because paraffin in the present composite maintains its thermal performances perfectly and therefore present higher thermal storage capabilities.

The thermal stability and weight loss percentage of SiO_2, paraffin, and the paraffin@SiO_2 composite were studied by TGA measurements, and the TGA curves are shown in Figure 5. For SiO_2, there is only a step of weight loss below 100 °C, and the weight loss is about 4%, which can be ascribed to the removal of absorbed water. The pure paraffin starts to be removed at about 140 °C, and the final weight loss percentage is nearly 100% at 260 °C. In the TGA curve of the paraffin@SiO_2 composite, the weight loss at temperatures below 100 °C is typically associated with the evaporation of residual solvent and that at temperatures of 160−270 °C is attributed to the removal of paraffin in the paraffin@SiO_2 composite. The weight loss percentage corresponding to the removal of paraffin in the composite is about 32.5%, which is the loading content of paraffin in the microencapsulated paraffin@SiO_2 composite. It can be seen that the onset temperature for the weight loss of the composite is higher than that of the pure paraffin, and the temperature of the maximum weight loss of the composite is about 10 °C higher than that of the pure paraffin, meaning that the SiO_2 shells can improve the thermal stability of paraffin in the composite. The SiO_2 shells create a physical protective

dx.doi.org/10.1021/sc300082m | ACS Sustainable Chem. Eng. 2013, 1, 374−380

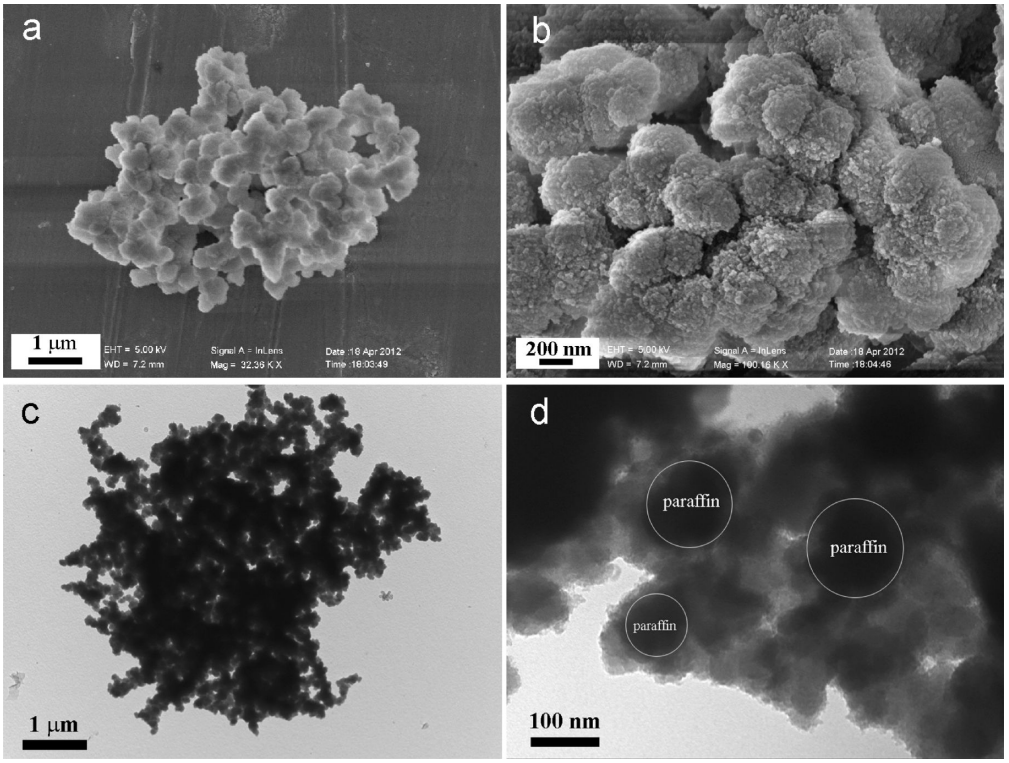

Figure 4. (a,b) SEM images and (c,d) TEM images of the microencapsulated paraffin@SiO_2 composite.

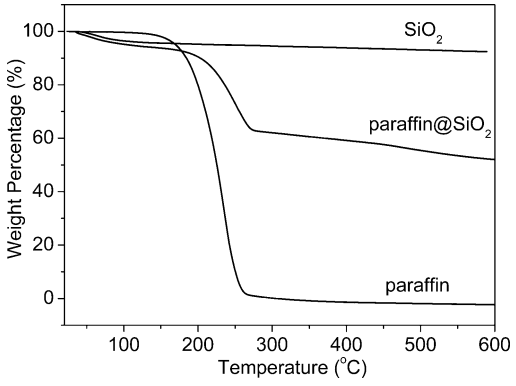

Figure 5. TGA curves of SiO_2, paraffin, and microencapsulated paraffin@SiO_2 composite.

barrier on the surface of the paraffin cores, which insulate the core material and slow the escape of the volatile products generated during thermal evaporation. Moreover, such a protective barrier can limit the transfer of flammable molecules to the gas phase and oxygen diffusion in the condensed phase,[30] meaning that the SiO_2 shells can improve the thermal stability and flame retardance of the composite due to the synergistic effect between the paraffin and SiO_2.

The phase change temperatures and latent heats of pure paraffin and the microencapsulated paraffin@SiO_2 composite were measured using differential scanning calorimeter (DSC). Figure 6a shows the melting–freezing DSC curves of pure paraffin and the paraffin@SiO_2 composite in the first phase change cycle. The phase change characteristics of the microencapsulated paraffin@SiO_2 composite are quite similar to those of the pure paraffin, which is because there is no chemical reaction between paraffin and SiO_2 in preparation of

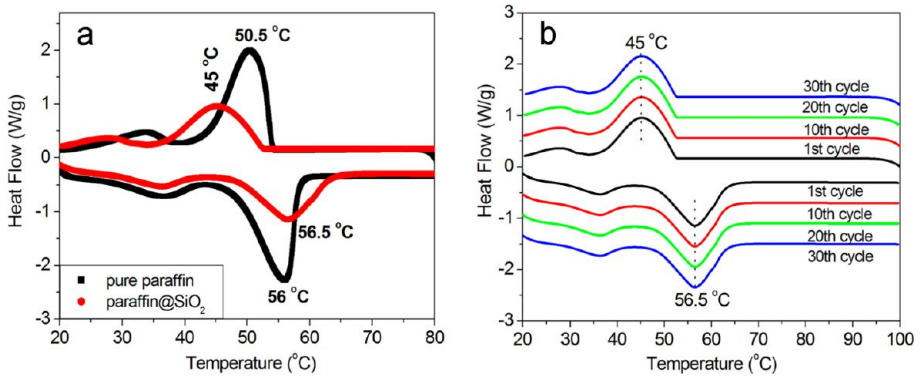

Figure 6. (a) Melting–freezing DSC curves for the first phase change cycle of paraffin and paraffin@SiO_2 composite. (b) DSC curves for 30 phase change cycles of paraffin@SiO_2 composite.

dx.doi.org/10.1021/sc300082m | ACS Sustainable Chem. Eng. 2013, 1, 374–380

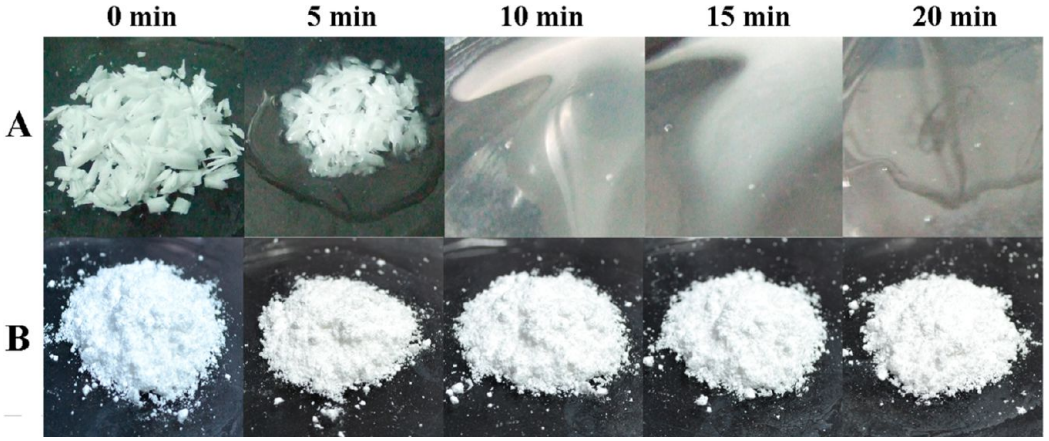

Figure 7. Photographs of pure paraffin (row A) and paraffin@SiO_2 composite (row B) heated at 70 °C for different times.

the paraffin@SiO_2 composite. For both of the samples, there are two endothermic peaks in the melting DSC curve and two exothermic peaks in the solidifying DSC curves. The small peaks represent the solid−solid transition process, and the main peaks denote the solid−liquid melting process or liquid−solid solidifying process. Before the melting, the solid−solid transition is induced by phase transformation from an ordered phase to a more disordered rotator phase. From Figure 6a, the solid−liquid melting peak and liquid−solid freezing peak were used to calculate the melting and freezing latent heat values, respectively. The melting and freezing temperatures are measured to be 56.0 and 50.5 °C for the paraffin and 56.5 and 45 °C for paraffin@SiO_2 composite, respectively. The melting and freezing latent heats are measured to be 143.5 and 144 J/g for the pure paraffin and 45.5 and 43.8 J/g for the composite, respectively. It is observed that the endothermic/exothermic peaks of the paraffin@SiO_2 composite shift toward higher/lower temperatures and become wider compared with those of pure paraffin. As reported previously, the encapsulation can result in a heterogeneous nucleating effect of the silica inner wall on the crystallization of paraffin,[24,28,31] which leads to an increase/decrease in the melting/freezing temperatures and a wideness of the temperature range for the phase transitions. Figure 6b shows the DSC curves during 30 phase change cycles of the paraffin@SiO_2 composite. The DSC curves of 30 phase change cycles fully coincide, and the phase change temperature and latent heat are identical in each melting−solidifying cycle, indicating that the sample has a good cycle performance of phase transition. In addition, the seepage test above the melting temperature of paraffin has been carried out to demonstrate the form-stable performance of the as-prepared composite. Figure 7 shows the photographs of pure paraffin and the paraffin@SiO_2 composite heated at 70 °C for different time. As seen from the photographs, the pure paraffin completely melted into liquid after being heated at 70 °C for 10 min. Whereas, the paraffin@SiO_2 composite kept its form of dry powder during the whole heating process, and no liquid leaked from the sample. The result of the seepage test confirms that the SiO_2 shells provide mechanical strength for the microencapsulated composite and prevent the seepage of the melted paraffin.

As one of the most important phase change performances affecting the working effect of the composite PCMs, the phase change enthalpy strongly depends on the encapsulation ratio and encapsulation efficiency of paraffin microencapsulated in SiO_2. The encapsulation ratio (R) and encapsulation efficiency (E) can be calculated by the results of the DSC measurements and according to eqs 3 and 4, respectively.[24]

$$R = \frac{\Delta H_{m,Composite}}{\Delta H_{m,Paraffin}} \times 100\% \quad (3)$$

$$E = \frac{\Delta H_{m,Composite} + \Delta H_{f,Composite}}{\Delta H_{m,Paraffin} + \Delta H_{f,Paraffin}} \times 100\% \quad (4)$$

where $\Delta H_{m,Composite}$ and $\Delta H_{f,Composite}$ represent the melting and freezing latent heat of the microencapsulated composite, respectively. $\Delta H_{m,Paraffin}$ and $\Delta H_{f,Paraffin}$ are the melting and freezing latent heat of the pure paraffin, respectively. The encapsulation ratio of paraffin in the composite was calculated to be 31.7%, slightly lower than the loading content (32.5%) of paraffin in the microencapsulated composite from the TGA measurements. It is worth noting that the encapsulation ratio describes the effective encapsulation of paraffin in the paraffin@SiO_2 composite, while the loading content is considered as the total weight percent of paraffin in the composite. It is understandable that not all the paraffin in the composite can perform the thermal storage/release performance of the PCMs. Therefore, the encapsulation ratio represents the effective performance of the paraffin in the paraffin@SiO_2 composite for heat energy storage. Besides, the encapsulation efficiency is calculated as 31.1% by the enthalpies involved in both of the melting and freezing processes, which is more suitable to evaluate the working efficiency of the paraffin@SiO_2 composite than the encapsulation ratio. To intuitively evaluate the capability that paraffin in the composite can perform the thermal storage/release performance, the thermal storage capability (η) of the paraffin@SiO_2 composite is determined by eq 5

$$\eta = \frac{\frac{\Delta H_{m,Composite} + \Delta H_{f,Composite}}{R}}{\Delta H_{m,Paraffin} + \Delta H_{f,Paraffin}} \times 100\% \quad (5)$$

As a result, the thermal storage capability of the microencapsulated paraffin in the composite is calculated as 98%. Compared with the microencapsulated palmitic acid@AlOOH reported previously,[16] the present paraffin@SiO_2 composite exhibits a much higher thermal storage capability in spite of its lower encapsulated ratio of paraffin in the composite.

The thermal storage/release performances of pure paraffin and the paraffin@SiO_2 composite were investigated in the

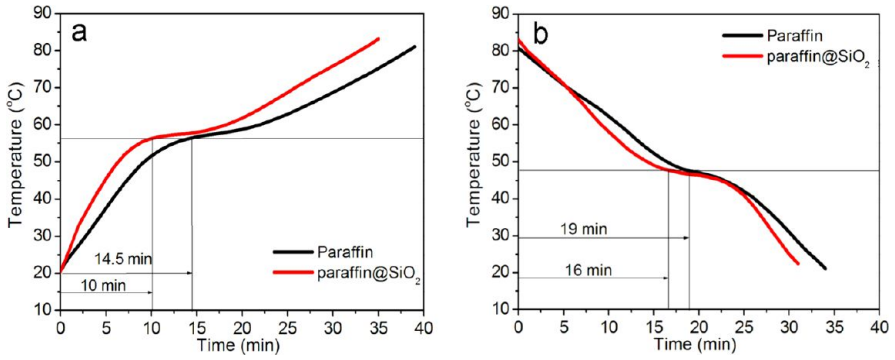

Figure 8. Temperature–time curves for (a) melting process and (b) freezing process of pure paraffin and the microencapsulated paraffin@SiO_2 composite.

range of 20–80 °C, using the constant temperature water bath method. The temperature–time curves for melting and freezing process are shown in Figure 8. There are temperature plateaus during both the heating and cooling process, which come from the phase transition of the PCM. During the heating process (Figure 8a), it took 14.5 min for pure paraffin to raise the temperature from room temperature (about 20 °C) to the temperature plateau of 56 °C but only 10 min for the microencapsulated paraffin@SiO_2 composite. During the cooling process (Figure 8b), the temperature achieved the plateau at about 47 °C when the time reached 16 min for the composite, whereas that for paraffin is about 19 min. Compared with pure paraffin, the composite reached the temperature plateaus in a shorter time, indicating that the thermal storage/release rates were increased by introducing inorganic SiO_2 shells.

CONCLUSION

A novel microencapsulated paraffin@SiO_2 composite PCM was successfully prepared by an in situ emulsion interfacial hydrolysis and polycondensation process. In the composite, paraffin was used as the core material for thermal energy storage, and SiO_2 acted as the shell material for improving the thermal stability of the microencapsulated composites. The melting temperature and latent heat of the composite were determined as 56.5 and 45.5 J/g by DSC, respectively. The phase change characteristics of the microencapsulated paraffin@SiO_2 composite are close to those of the pure paraffin because there is no chemical reaction between paraffin and SiO_2 in preparation of the composite. The composite with a paraffin encapsulation ratio of 31.7 wt % could maintain its phase transition perfectly after subjected to 30 melting–freezing cycles, and no leakage of paraffin was observed at 70 °C for 20 min. The as-prepared composite has a high heat storage capability and good thermal stability, indicating that the composite can be used as a potential material to store thermal energy in practical application. The method and mechanism for preparing the present microencapsulated paraffin@SiO_2 composite PCM can be extended to fabricate other organics@inorganics PCMs with different core/shell compositions.

AUTHOR INFORMATION

Corresponding Author

*Tel: +86-554-6668649. Fax: +86-554-6668643. E-mail: libx@mail.ustc.edu.cn.

Notes

The authors declare no competing financial interest.

ACKNOWLEDGMENTS

We thank Dr. Jinbao Zhu of University of Science & Technology of China for his help with the sample characterization and good suggestions in the results' analysis. This work was financially supported by the National Natural Science Foundation of China (21001003), National Basic Research Program of China (2009CB939901), and Excellent Young and Middle-aged Backbone Teachers Fund of Anhui University of Science and Technology.

REFERENCES

(1) Agyenim, F.; Hewitt, N.; Eames, P. A review of materials, heat transfer and phase change problem formulation for latent heat thermal energy storage systems (LHTESS). *Renewable Sustainable Energy Rev.* **2010**, *14*, 615–628.

(2) Li, M.; Wu, Z. S.; Tan, J. M. Properties of form-stable paraffin/silicon dioxide/expanded graphite phase change composites prepared by sol–gel method. *Appl. Energy* **2012**, *92*, 456–461.

(3) Fang, X. M.; Zhang, Z. G.; Chen, Z. H. Study on Preparation of montmorillonite-based composite phase change materials and their applications in thermal storage building materials. *Energy Convers. Manage.* **2008**, *49*, 718–723.

(4) Zalba, B.; Martin, J. M.; Cabeza, L. F.; Mehling, H. Review on thermal energy storage with phase change: Materials, heat transfer analysis and applications. *Appl. Therm. Eng.* **2003**, *23*, 251–283.

(5) Sharma, A.; Tyagi, V. V.; Chen, C. R.; Buddhi, D. Review on thermal energy storage with phase change materials and applications. *Renewable Sustainable Energy Rev.* **2009**, *13*, 318–345.

(6) Guillot, S.; Faik, A.; Rakhmatullin, A.; Lambert, J.; Veron, E.; Echegut, P.; Bessada, C.; Calvet, N.; Py, X. Corrosion effects between molten salts and thermal storage material for concentrated solar power plants. *Appl. Energy* **2012**, *94*, 174–181.

(7) Najjar, A.; Hasan, A. Modeling of greenhouse with PCM energy storage. *Energ. Convers. Manage* **2008**, *49*, 3338–3342.

(8) Mondal, S. Phase change materials for smart textiles – An overview. *Appl. Therm. Eng.* **2008**, *28*, 1536–1550.

(9) Jaworski, M. Thermal performance of heat spreader for electronics cooling with incorporated phase change material. *Appl. Therm. Eng.* **2012**, *35*, 212–219.

(10) Kousksou, T.; Jamil, A.; ElRhafiki, T.; Zeraouli, Y. Paraffin wax mixtures as phase change materials. *Sol. Energy Mater. Sol. Cells* **2010**, *94*, 2158–2165.

(11) Ehid, R.; Fleischer, S. A. Development and characterization of paraffin-based shape stabilized energy storage materials. *Energy Convers. Manage.* **2012**, *53*, 84–91.

(12) Zhang, Z. G.; Zhang, N.; Peng, J.; Fang, X. M.; Gao, X. N.; Fang, Y. T. Preparation and Thermal energy storage properties of paraffin/

expanded graphite composite phase change material. *Appl. Energy* **2012**, *91*, 426−431.
(13) Li, M.; Kao, H. T.; Wu, Z. S.; Tan, J. M. Study on preparation and thermal property of binary fatty acid and the binary fatty acids/diatomite composite phase change materials. *Appl. Energy* **2011**, *88*, 1606−1612.
(14) Su, J. F.; Wang, X. Y.; Wang, S. B.; Zhao, Y. H.; Huang, Z. Fabrication and properties of microencapsulated-paraffin/gypsum-matrix building materials for thermal energy storage. *Energ. Convers. Manage* **2012**, *55*, 101−107.
(15) Fang, G. Y.; Chen, Z.; Li, H. Synthesis and properties of microencapsulated paraffin composites with SiO_2 shell as thermal energy storage materials. *Chem. Eng. J.* **2010**, *163*, 154−159.
(16) Pan, L.; Tao, Q. H.; Zhang, S. D.; Wang, S. S.; Zhang, J.; Wang, S. H.; Wang, Z. Y.; Zhang, Z. P. Preparation, characterization and thermal properties of micro-encapsulated phase change materials. *Sol. Energy Mater. Sol. Cells* **2012**, *98*, 66−70.
(17) Li, J. L.; Xue, P.; Ding, W. Y.; Han, J. M.; Sun, G. L. Micro-encapsulated paraffin/high-density polyethylene/wood flour composite as form-stable phase change material for thermal energy storage. *Sol. Energy Mater. Sol. Cells* **2009**, *93*, 1761−1767.
(18) Farid, M. M.; Khudhair, A. M.; Razack, S.; Al-Hallaj, S. A review on phase change energy storage: materials and applications. *Energy Convers. Manage.* **2004**, *45*, 1597−1615.
(19) Teixeira, M. I.; Andrade, L. R.; Farina, M.; Rocha-Leao, M. M. Characterization of short chain fatty acid microcapsules produced by spray drying. *Mater. Sci. Eng., C* **2004**, *24*, 653−658.
(20) Li, W.; Song, G. L.; Tang, G. Y.; Chu, X. D.; Ma, S. D.; Liu, C. F. Morphology, structure and thermal stability of microencapsulated phase change material with copolymer shell. *Energy* **2011**, *36*, 785−791.
(21) Bao, Y.; Pan, W.; Wang, T.; Wang, Z.; Wei, F.; Xiao, F. Microencapsulation of fatty acid as phase change material for latent heat storage. *J. Energy Eng.* **2011**, *137*, 214−219.
(22) Li, W.; Zhang, X. X.; Wang, X. C.; Niu, J. J. Preparation and characterization of microencapsulated phase change material with low remnant formaldehyde content. *Mater. Chem. Phys.* **2007**, *106*, 437−442.
(23) Su, J.; Wang, L.; Ren, L. Fabrication and thermal properties of microPCMs: Used melamine-formaldehyde resin as shell material. *J. Appl. Polym. Sci.* **2006**, *101*, 1522−1528.
(24) Zhang, H.; Wang, X.; Wu, D. Silica encapsulation of n-octadecane via sol-gel process: A novel microencapsulated phase change material with enhanced thermal conductivity and performance. *J. Colloid Interface Sci.* **2010**, *343*, 246−255.
(25) Borreguero, A. M.; Valverde, J. L.; Rodríguez, J. F.; Barber, A. H.; Cubillo, J. J.; Carmona, M. Synthesis and characterization of microcapsules containing rubitherm®RT27 obtained by spray drying. *Chem. Eng. J.* **2011**, *166*, 384−390.
(26) Karaipekli, A.; Sari, A. Capric−myristic acid/expanded perlite composite as form-stable phase change material for latent heat thermal energy storage. *Renw. Energy* **2008**, *33*, 2599−2605.
(27) Mei, D. D.; Zhang, B.; Liu, R. C.; Zhang, H. Q.; Liu, J. D. Preparation of stearic acid/halloysite nanotube composite as form-stable PCM for thermal energy storage. *Int. J Energy Res* **2011**, *35*, 828−834.
(28) Zhang, H. Z.; Wang, X. D. Synthesis and properties of microencapsulated n-octadecane with polyurea shells containing different soft segments for heat energy storage and thermal regulation. *Sol. Energy Mater. Sol. Cells* **2009**, *93*, 1366−1376.
(29) Li, H.; Fang, G. Y.; Liu, X. Synthesis of shape-stabilized paraffin/silicon dioxide composites as phase change material for thermal energy storage. *J. Mater. Sci.* **2010**, *45*, 1672−1676.
(30) Zhang, P.; Hua, Y.; Song, L.; Lua, H. D.; Wang, J.; Liu, Q. Q. Synergistic effect of iron and intumescent flame retardant on shape-stabilized phase change material. *Thermochim. Acta* **2009**, *487*, 74−79.
(31) Gong, C. Y.; Zhang, H. Z.; Wang, X. D. Effect of shell materials on microstructure and properties of microencapsulated n-octadecane. *Iran. Polym. J.* **2009**, *18*, 501−512.